Role of Inelastic Tunneling through the Insulating Barrier in Scanning-Tunneling-Microscope Experiments on Cuprate Superconductors

S. Pilgram, T. M. Rice, and M. Sigrist
Theoretische Physik, ETH Zurich, CH-8093 Zürich, Switzerland
(Received 26 May 2006; published 15 September 2006)

The tunneling path between the CuO_2 layers in cuprate superconductors and a scanning-tunneling-microscope tip passes through a barrier made from other oxide layers. This opens up the possibility that inelastic processes in the barrier contribute to the tunneling spectra. Such processes cause one or possibly more peaks in the second derivative current-voltage spectra displaced by phonon energies from the density of states singularity associated with superconductivity. Calculations of inelastic processes generated by apical O phonons show good qualitative agreement with recent experiments reported by Lee *et al.* Further tests to discriminate between these inelastic processes and coupling to planar phonons are proposed.

DOI: 10.1103/PhysRevLett.97.117003 PACS numbers: 74.72.−h, 68.37.Ef, 74.25.Kc, 74.50.+r

The importance of the electron-phonon interaction in the high temperature cuprate superconductors has long been a matter of debate. In conventional superconductors tunneling experiments analyzed by McMillan and Rowell [1] not only unequivocally established that the exchange of phonons between electrons is the underlying mechanism for Cooper pairing but also allowed its spectroscopic determination. In the case of cuprates there are many good reasons to doubt the dominance of an attraction due to phonon exchange. These reasons range from the d-wave rather than s-wave pairing symmetry, to their electronic structure as lightly doped Mott insulators. The latter points toward a strong on-site Coulomb repulsion which cannot be treated perturbatively, violating a key postulate in the standard BCS-Eliashberg theory. A number of proposals have been made for a subdominant role for the electron-phonon interactions particularly involving the half-buckling phonon modes which couple attractively in the d-wave pairing channel [2–7].

Very recently, a new set of tunneling measurements at low temperatures has been reported by Lee *et al.* [8] using a scanning-tunneling microscope (STM). Results with this local tunneling probe show considerable variations in the form and energy of the density of states (DOS) singularity associated with the superconductivity and also a peak in the second derivative current-voltage spectra which is displaced from the DOS peak by a fairly constant energy. Lee *et al.* [8] report further that isotope substitution on the O ions shifts this energy consistent with a phonon origin for this peak. This raises the question whether these spectra should be interpreted analogously to those of conventional superconductors or if these peaks have another source.

A series of works explain the appearance of side peaks in the DOS of d-wave superconductors in terms of localized bosonic modes [9], resonant spin modes [10,11], or the breathing mode phonons [12]. All these proposals consider inelastic processes that happen directly in the superconducting plane. In this Letter we examine an alternative explanation in terms of inelastic processes in the tunneling barrier. Such inelastic processes are well established in electron tunneling spectroscopy [13–16] of metal-insulator-metal junctions and in STM spectra taken on metals with adsorbed molecules [17,18]. In cleaved BSSCO the topmost layer is the BiO plane, but the electrons tunnel into and out of the CuO_2 planes. Inelastic tunneling can occur in the intervening barrier, e.g., when the tunneling hole passes through the apical O ion. Although the $2p_z$ orbitals of the apical O ion do not hybridize with the $3d_{x^2-y^2}$ orbitals of the Cu ion directly below there is a weaker hybridization with orbitals centered on neighboring Cu ions [19]. However, we will not go into such details here. Rather, we examine a simple model which has an important tunneling path through an apical O orbital removed from the chemical potential. This tunneling path is in turn coupled to a vibration of this ion. Our aim is to establish the key features of this inelastic process in the tunneling barrier and to compare them to the experimental spectra.

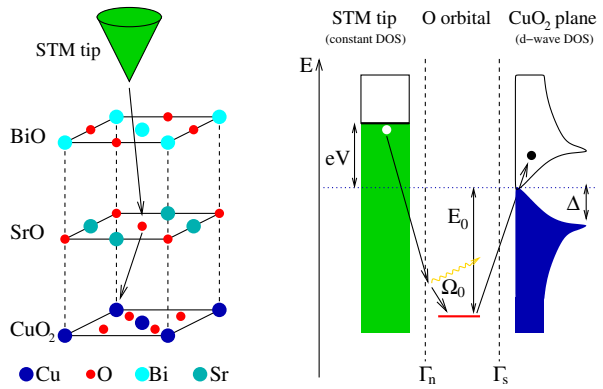

FIG. 1 (color online). Left panel: geometry relevant for the scanning-tunneling-microscope experiment; the superconducting CuO_2 plane lies below BiO and SrO layers. Right panel: suggested inelastic cotunneling process via the apical oxygen atom leading to phonon satellites in the current-voltage characteristics in electron-energy scheme.

Our aim is to calculate the cotunneling current through the $2p_z$ orbital of the apical O ion. For this purpose we describe the setup depicted in Fig. 1 by the Hamiltonian,

$$H = H_n + H_s + H_t + E_0 \sum_s p_s^\dagger p_s + \sum_q \omega_q b_q^\dagger b_q + \sum_{qs} M_q p_s^\dagger p_s (b_q + b_{-q}^\dagger). \quad (1)$$

The first term H_n represents the normal conducting STM tip, characterized by a constant DOS. The second term H_s stands for the superconducting CuO_2 plane. We assume for simplicity a d-wave-type DOS $N_s(\varepsilon) \propto \langle \mathrm{Re}[\varepsilon/\sqrt{\varepsilon^2 - \Delta^2 \cos^2\theta}]\rangle_\theta$. However, in the experiment [8] the shape of the superconducting DOS varies strongly from point to point. The third term H_t describes the hopping onto the apical oxygen orbital from both the STM tip and the CuO_2 plane. Partial linewidths Γ_n, Γ_s of the $2p_z$ orbital are used to describe its hybridization with the STM tip and the superconducting CuO_2 plane. The fourth term in Eq. (1) defines the energy E_0 of a hole in the oxygen p orbital which is created by the operator $p_s^\dagger$. The fifth term in Eq. (1) includes the phonon dispersion ω_q; the operator $b_q^\dagger$ creates a phonon with momentum q. Since the phonon involves mainly the motion of the apical oxygen atoms we assume an optical phonon band centered around frequency Ω_0 with a weak dispersion (i.e., a small bandwidth W). The last term in Eq. (1) finally describes the coupling of the oxygen p orbital to the phonons via the coupling constant M_q.

As we shall discuss at the end of this section the parameters Γ_n, Γ_s, and E_0 mainly affect the overall prefactor in the tunneling current and are not very crucial. The shape of the current-voltage characteristics is determined by the DOS of the superconductor, N_s, and the phonon spectrum, ω_q.

The derivation of the cotunneling current follows closely Ref. [20] which deals with a similar nonequilibrium situation in the normal conducting state. Tunneling is treated to lowest order, while electron-phonon coupling is treated nonperturbatively allowing for multiphonon processes. Applying a Lang-Firsov transformation [21] and standard manipulations of many-body physics [22] one arrives at the following expression for the cotunneling current (we set $\hbar = 1$)

$$I(V) = \frac{e\Gamma_n\Gamma_s}{2\pi} \int \frac{F_n(\varepsilon)\bar{F}_s(\varepsilon) - F_s(\varepsilon)\bar{F}_n(\varepsilon)}{(\varepsilon - E_0)^2 + |\Sigma(\varepsilon)|^2} d\varepsilon. \quad (2)$$

The factors $F_x(\varepsilon)$, $\bar{F}_x(\varepsilon)$ with $x = n, s$ are obtained from a convolution,

$$\begin{pmatrix} F_x(\varepsilon) \\ \bar{F}_x(\varepsilon) \end{pmatrix} = \int d\omega n_x(\varepsilon + \omega) \begin{pmatrix} B(\omega) f_x(\varepsilon + \omega) \\ B(-\omega)[1 - f_x(\varepsilon + \omega)] \end{pmatrix}, \quad (3)$$

of the relevant normalized DOS, $n_n(\varepsilon) = 1$ or $n_s(\varepsilon) = \langle \mathrm{Re}[\varepsilon/\sqrt{\varepsilon^2 - \Delta^2\cos^2\theta}]\rangle_\theta$, and the corresponding Fermi factors, $f_n(\varepsilon)$ or $f_s(\varepsilon)$, with the phonon correlation function $B(\omega)$. The latter will be discussed in detail below. The retarded self-energy $\Sigma(\varepsilon)$ of the $2p_z$ orbital reads

$$\Sigma(\varepsilon) = -\frac{i}{2} \sum_{x=n,s} \Gamma_x \{F_x(\varepsilon) + \bar{F}_x(\varepsilon)\}. \quad (4)$$

If the energy E_0 of the virtual oxygen state is the largest energy scale in the problem, the energy dependence of the denominator of Eq. (2) can be neglected [23]. In this case, we may approximate the tunneling current by

$$I(V) \sim \int \{F_n(\varepsilon)\bar{F}_s(\varepsilon) - F_s(\varepsilon)\bar{F}_n(\varepsilon)\} d\varepsilon \quad (5)$$

and the parameters E_0, Γ_n, Γ_s describing the virtual state enter only in the (unimportant) prefactor. Even if terms with $\varepsilon \simeq E_0$ contribute significantly to the integral (2), the energy dependence of the denominator will only lead to an asymmetry of the current-voltage signal on a larger energy scale. In the following, we therefore concentrate on the influence of the phonon spectrum which creates the sharp features visible in the experiment [8].

The phonon spectrum enters the current-voltage spectrum (2) via the modified occupation factors (3). In Eq. (3), the phonon correlation function $B(\omega) = (2\pi)^{-1} \times \int dt e^{i\omega t} \langle X(t) X^\dagger(0)\rangle$ describes possible phonon emission or absorption of the oxygen $2p_z$ orbital. Those processes lead to an effective shift of the Fermi occupation factors of both the superconducting plane and the normal conducting STM tip. The "displacement" operator $X = \exp\{\sum_q M_q (b_q - b_{-q}^\dagger)/\omega_q\}$ results from a Lang-Firsov transformation [21]. Replacing the q summation by a frequency integration over a box density of states and assuming zero temperature for the phonon bath we obtain the correlation function

$$\langle X(t) X^\dagger(0)\rangle = \exp\left\{\lambda^2 \left(\frac{2}{Wt} \sin\frac{Wt}{2} e^{-i\Omega_0 t} - 1\right)\right\} \quad (6)$$

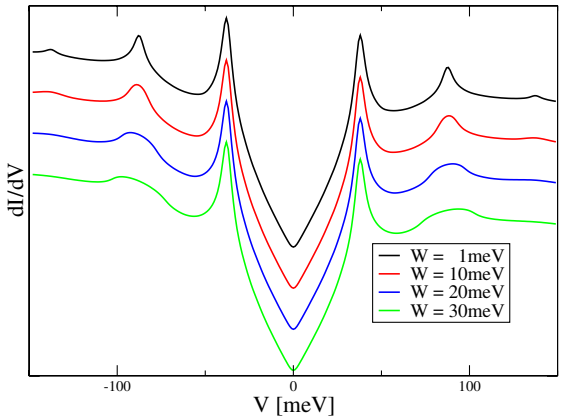

FIG. 2 (color online). Shape of dI/dV for different widths W of the phonon band. Parameters are $\Delta = 38$ meV, $\Omega_0 = 50$ meV, $\lambda = 0.4$, $E_0 = 2$ eV.

which is used in the following numerical calculations. The parameter λ measures the strength of electron-phonon coupling, Ω_0 is the mean phonon frequency, and W defines the bandwidth. Note that this correlation function takes into account multiple phonon emissions. A purely perturbative treatment corresponds to the expansion of the exponential in Eq. (6) to quadratic order in the coupling constant λ.

Figure 2 shows the differential tunneling conductance dI/dV for different widths of the optical phonon band. The phonon satellites are most clearly visible in the case of completely localized Einstein phonons ($W = 1$ meV). Each satellite then reproduces exactly the singularity of the quasiparticle peak in the superconducting DOS. The case of Einstein phonons seems to be excluded by the experimental data which shows broadened phonon satellites. Comparing qualitatively peak heights and peak widths of theory and experiment, we are led to the conclusion that the phonon band has a width of roughly 20 meV. This width is probably due to the vibrational coupling of the apical oxygen atom to its neighbors. Since the electron-phonon coupling constant is quite large one might also expect broadening due to particle-hole excitations in the superconducting plane or due to the anharmonicity of the crystal leading to a finite phonon lifetime.

In Fig. 3 we show the dependence of the differential conductance on the electron-phonon coupling strength λ. The stronger the coupling the more phonon satellites become visible in the spectrum. The amplitude of the nth satellite is smaller than that of the $n-1$th satellite by roughly a factor of λ^2/n. A comparison of first and second satellite therefore allows for an estimate of the coupling strength λ. From the experimental data we estimate $\lambda \simeq 0.4$.

Figure 4 evaluates the isotope effect in the second derivative d^2I/dV^2 of the current-voltage spectrum as measured in the experiment [8]. The isotope effect is most clearly visible for the first satellite which stems from a single convolution of the quasiparticle peak with the phonon spectrum. The second satellite stems from a twofold convolution with the phonon spectrum. Its second derivative d^2I/dV^2 is therefore much smoother, and the isotope effect less well seen.

Experimentally [8], the lowest phonon frequency is obtained as the energy difference between the quasiparticle peak in the dI/dV (in our case at 38 meV) and the maximum of the second derivative d^2I/dV^2 (in our case at 78 meV). This procedure is standard in conventional superconductivity where the strong singularity in the s-wave density of states guarantees a pronounced feature in the second derivative d^2I/dV^2. In the case of d-wave superconductivity this singularity is much weaker and consequently the maxima in the second derivative are less well defined. If the quasiparticle peak is weakened or if the second phonon satellite is investigated another procedure to determine the phonon frequencies can be preferable: determining the positions of both maximum and minimum in the second derivative and taking their average one can directly estimate the central frequency of the phonon band.

Inelastic processes in the tunneling barrier show up as a pronounced peak in the d^2I/dV^2 spectrum displaced by a phonon energy from the main peak in the dI/dV associated with the DOS singularity which accompanies d-wave superconductivity. The strength and form of the peak reflects those of the DOS singularity. This feature agrees with experiments of Lee *et al.* [8]. A weaker signal also appears displaced by twice the phonon energies in agreement with experiment. The phonon energy, 50 meV, chosen to agree with the experimental spectra, is close to the value expected for an apical O phonon and rather higher than the energy of the B_{1g} half-buckling mode [25]. One point of divergence between the theory and the spectra reported by Lee *et al.* is the presence of a sharp minimum in the calculated d^2I/dV^2 spectra just above the peak.

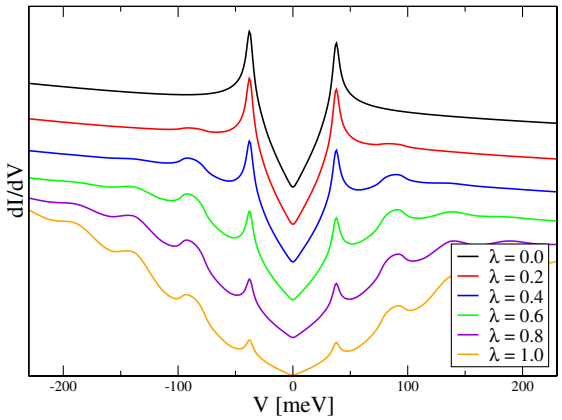

FIG. 3 (color online). Shape of dI/dV for different electron-phonon couplings λ. Parameters are $\Delta = 38$ meV, $\Omega_0 = 50$ meV, $W = 20$ meV, $E_0 = 2$ eV.

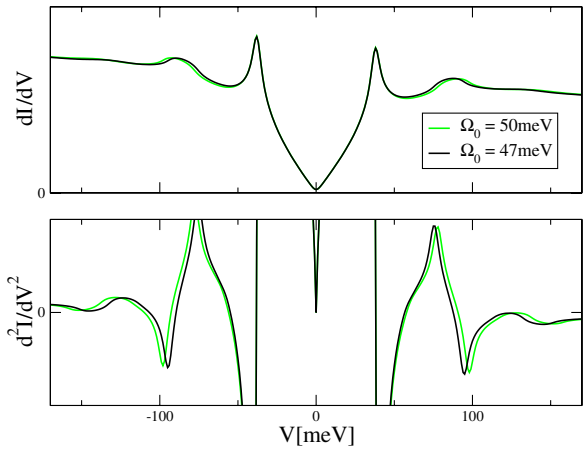

FIG. 4 (color online). Isotope shift in the d^2I/dV^2. Parameters are $\Delta = 38$ meV, $\Omega_0 = 50$ meV, $W = 20$ meV, $\lambda = 0.4$, $E_0 = 2$ eV. The sign in the d^2I/dV^2 for negative voltages has been flipped.

The STM experiments of Lee *et al.* [8] show substantial spatial variations in the spectra with a clear correlation between the frequency shift of the side peaks and the local value of the superconducting energy gap. Such a correlation follows if the local bosonic mode couples directly to the planar holes and if this electron-boson coupling is involved in the superconductivity. In our model, unlike those of Refs. [9–12], such an explanation does not apply. However, it is known empirically that the positions of the apical O ions influences the transition temperature T_c of BSSCO superconductors [26] and more generally that materials with longer Cu-apical O bonds have higher values of T_c [27,28]. Therefore, the anticorrelation between the local magnitude of the superconducting gap and the local size of the frequency shift may reflect this empirical trend and is not incompatible with our model which ascribes these side peaks to inelastic processes in the tunneling barrier.

Lee *et al.* [8] report an isotope shift when all O sites are occupied by O^{16} versus O^{18}. A selective isotope replacement only on the apical O sites would discriminate between our proposal that the structure is due to apical O phonons rather than due to the half-buckling mode involving displacements of planar O ions.

In summary, we conclude that inelastic tunneling processes involving the apical O ions are a viable explanation of the phononic structure in the STM tunneling spectra recently observed by Lee *et al.* and we propose selective isotope substitution as a test of our proposal.

We thank J. C. Davis, A. V. Balatsky, and the authors of Ref. [8] for sharing their data with us in advance of publication and F. C. Zhang, C. Honerkamp, and D. J. Scalapino for stimulating discussions. We acknowledge support from the Swiss National Science Foundation and from the MaNEP (Materials with Novel Electronic Properties) program.

[1] W. L. McMillan and J. M. Rowell, in *Superconductivity*, edited by R. D. Parks (Dekker, New York, 1969), Vol. 1, p. 561.
[2] N. Bulut and D. J. Scalapino, Phys. Rev. B **54**, 14 971 (1996).
[3] T. Dahm, D. Manske, D. Fay, and L. Tewordt, Phys. Rev. B **54**, 12 006 (1996).
[4] T. S. Nunner, J. Schmalian, and K. H. Bennemann, Phys. Rev. B **59**, 8859 (1999).
[5] A. Nazarenko and E. Dagotto, Phys. Rev. B **53**, R2987 (1996).
[6] O. Jepsen *et al.*, J. Phys. Chem. Solids **59**, 1718 (1998).
[7] C. Honerkamp, H. C. Fu, and D. H. Lee, cond-mat/0605161.
[8] J. Lee, K. Fujita, K. McElroy, J. A. Slezak, M. Wang, Y. Aiura, H. Bando, M. Ishikado, T. Masui, J.-X. Zhu, A. V. Balatsky, H. Eisaki, S. Uchida, and J. C. Davis, Nature (London) **442**, 546 (2006).
[9] D. K. Morr and R. H. Nyberg, Phys. Rev. B **68**, 060505(R) (2003).
[10] A. V. Balatsky, Ar. Abanov, and J.-X. Zhu, Phys. Rev. B **68**, 214506 (2003).
[11] J.-X. Zhu, J. Sun, Q. Si, and A. V. Balatsky, Phys. Rev. Lett. **92**, 017002 (2004).
[12] J.-X. Zhu, A. V. Balatsky, T. P. Devereaux, Q. Si, J. Lee, K. McElroy, and J. C. Davis, Phys. Rev. B **73**, 014511 (2006).
[13] R. C. Jaklevic and J. Lambe, Phys. Rev. Lett. **17**, 1139 (1966).
[14] D. J. Scalapino and S. M. Marcus, Phys. Rev. Lett. **18**, 459 (1967).
[15] J. Kirtley and P. K. Hansma, Phys. Rev. B **13**, 2910 (1976).
[16] J. Kirtley, D. J. Scalapino, and P. K. Hansma, Phys. Rev. B **14**, 3177 (1976).
[17] X. H. Qiu, G. V. Nazin, and W. Ho, Phys. Rev. Lett. **92**, 206102 (2004).
[18] N. A. Pradhan, N. Liu, and W. Ho, J. Phys. Chem. B **109**, 8513 (2005).
[19] Y. Chen, T. M. Rice, and F. C. Zhang, cond-mat/0604190.
[20] L. Sheng, D. Y. Xing, and D. N. Sheng, Phys. Rev. B **70**, 094416 (2004).
[21] I. G. Lang and Y. A. Firsov, Zh. Eksp. Teor. Fiz. **43**, 1843 (1962) [Sov. Phys. JETP **16**, 1301 (1962)].
[22] G. D. Mahan, *Many-Particle Physics* (Plenum, New York, 1990).
[23] The energy E_0 needed to create a hole on the $2p_z$ orbital of the apical oxygen is typically of the order of 2 eV [24].
[24] Y. Ohta, T. Tohyama, and S. Maekawa, Phys. Rev. B **43**, 2968 (1991).
[25] W. Meevasana, N. J. C. Ingle, D. H. Lu, J. R. Shi, F. Baumberger, K. M. Shen, W. S. Lee, T. Cuk, H. Eisaki, T. P. Devereaux, N. Nagaosa, J. Zaanen, and Z.-X. Shen, Phys. Rev. Lett. **96**, 157003 (2006).
[26] H. Eisaki, N. Kaneko, D. L. Feng, A. Damascelli, P. K. Mang, K. M. Shen, Z.-X. Shen, and M. Greven, Phys. Rev. B **69**, 064512 (2004).
[27] See Ref. [23] in Eisaki *et al.* [26].
[28] E. Pavarini, I. Dasgupta, T. Saha-Dasgupta, O. Jepsen, and O. K. Andersen, Phys. Rev. Lett. **87**, 047003 (2001).